

Schrödinger Spacetimes with Screen and Reduced Entanglement

Harvendra Singh

*Theory Division
Saha Institute of Nuclear Physics
1/AF Bidhannagar, Kolkata 700064, India*

Abstract

We study a particular class of type II string vacua which become Schrödinger like spacetime in the IR region but are conformally AdS in asymptotic UV region. These solutions are found to possess some unique properties such as the presence of a spacetime ‘screen’. This Schrödinger (spacetime) screen is however very different from a black-hole horizon. It requires the presence of finite chemical potential and a negative charge density in the Schrödinger CFT. We find that these vacua give rise to reduced entanglement entropy as compared to Lifshitz-AdS counterpart, perhaps due to the screening effects.

1 Introduction

A steady progress [1]-[32] has been made towards understanding the string solutions which exhibit Lifshitz and Schrödinger type nonrelativistic symmetries. Particularly, in these solutions the time and space coordinates in the dual CFT scale *asymmetrically*. Some of these systems exhibit a non-fermi liquid or strange metallic behaviour at very low temperatures. These strange effects have been alluded to the fact that strongly correlated quantum systems might have hidden fermi surfaces [18, 19]. There are similar issues related to the entanglement of information in the quantum systems [30, 18]. The entanglement of the subsystems is a very common concept in quantum physics in general, including black-holes [31], as well as an entangled quantum EPR pair [32]. But when a strongly correlated system at critical point can be represented as a system living on the boundary of some bulk gravity theory, the subject becomes much more phenomenologically appealing. In such holographic cases the entanglement entropy of a subsystem in the boundary can be defined geometrically as the area of a minimal surface, lying within the bulk spacetime having specific boundary conditions [30].

Following an early work on $AdS_5 \times S^5$ and finding the Lifshitz solutions [6], we recently generalized that approach for all Dp -brane AdS vacua and obtained Lifshitz and Schrödinger like solutions in type II string theory [10].¹ These vacua exhibit a fixed amount of supersymmetry. Our primary focus in this work are particularly the Schrödinger-like Dp brane solutions [10]. They appear in various dimensions and have nontrivial dynamical exponents given by $a_{\text{sch}} = \frac{2}{p-5}$, which is negative for $p < 5$. These IR Schrödinger solutions can be said to be the least understood type vacua, at least if we ask the questions about the entanglement entropy of the boundary CFT. The special characteristic of these zero temperature solutions is that they involve a compact null direction, because of which one generally cannot trust these Schrödinger geometries for classical calculations in the bulk geometry. It is so because for a meaningful (nonrelativistic) Schrödinger CFT description to arise, such as described in [1, 2, 4], it requires the null lightcone coordinate to be compact. In this work, we study a new class of Schrödinger-like Dp -brane solutions, which are closely related to the solutions given in [10], thus keeping the essential facts unchanged. However, the method we employ is applicable to any other Schrödinger solution. We shall engineer our solutions such that they first become well behaved classical geometries, at least in some finite UV region, such that they could eventually be compactified. Our ultimate aim is to estimate the entanglement entropy of

¹As per our terminology, all the Lifshitz-like solutions we discuss in this paper will have appropriate conformal factors in front of the Lifshitz metric when viewed after the compactification. Thus we shall be discussing ‘conformally Lifshitz’ vacua all through. These give rise to scaling violations in the nonrelativistic CFT. The corresponding hyperscaling parameters are calculated in [10]. Thus our solutions are different from the Lifshitz solutions introduced in [3], or the solutions with light-like matter [5]. Similarly, the Schrödinger solutions also come with appropriate conformal factors.

the CFT living at the boundary of these Schrödinger vacua. The new solutions are such that they interpolate smoothly between “conformally Schrödinger” solutions in the IR and the “conformally AdS” spacetime in the UV. We demonstrate various properties of these classical solutions in both the regions. These interpolating solutions are then used to calculate the entanglement entropy of strip-like subsystem in the boundary CFT. In conclusion, we find that a Ryu-Takayangi entropy functional can be suitably defined. We must emphasize here that for the standard Schrödinger metric such as $a = 2$ [1, 2]

$$-\frac{(dx^+)^2}{z^4} + \frac{-dx^+ dx^- + d\vec{x}^2}{z^2} + \frac{dz^2}{z^2}$$

the Ryu-Takayanagi entanglement entropy cannot be defined. In these Galilean $a = 2$ vacua, x^- is a compact ‘null’ coordinate, and because of this we cannot find a spacelike extremal surface inside the bulk whose area would give the entanglement entropy. Particularly all constant x^+ (time) surfaces have vanishing area. We will avoid this situation altogether in this work.

The paper is planned as follows. In section-2 we first review interpolating Lifshitz-AdS Dp -brane vacua and some of the basic properties including the entanglement entropy. The expert reader can skip this section and directly shift to section-3. In the section-3, we construct ‘conformally Schrödinger’ solutions which asymptotically become ‘conformally AdS’ vacua. These solutions give rise to finite chemical potential and a (negative) charge density. This construction allows us to introduce a new concept of *Schrödinger spacetime screen*, for these asymptotically AdS solutions. We define the entanglement entropy for the interpolating solutions. It is found that the entanglement entropy is lower for Schrödinger-AdS cases as compared to the Lifshitz-AdS case, provided the global parameters are kept the same. Some numerical analysis is presented in section-4 to reinforce our conclusions. The summary is provided in the section-5.

2 Interpolating Lifshitz-AdS string vacua

We first review the interpolating Lifshitz like solutions [33] as these are close cousins of Schrödinger type solutions which we will be discussing in the next section. The Lifshitz Dp -brane solutions with eight supersymmetries are given as [10]

$$ds_{lif}^2 = R_p^2 z^{\frac{p-3}{p-5}} \left[\left\{ \frac{\beta^2}{z^{4/(p-5)}} (dx^-)^2 + \frac{-dx^+ dx^- + d\vec{x}_{(p-1)}^2}{z^2} + \frac{4}{(5-p)^2} \frac{dz^2}{z^2} \right\} + d\Omega_{(8-p)}^2 \right],$$

$$e^\phi = (2\pi)^{2-p} (g_{YM})^2 R_p^{3-p} z^{\frac{(7-p)(p-3)}{2(p-5)}} \quad (1)$$

with the $(p+2)$ -form RR-flux (for $p \neq 5$). Here β is an arbitrary parameter and it can also be absorbed by scaling the lightcone coordinates. Note that the metric component

$g_{--} > 0$, so x^- is a space-like coordinate while x^+ will be treated as the lightcone time. When $\beta = 0$ these solutions exactly become conformally AdS (for $p \neq 3$) string solutions which arise as the near horizon geometry of N coincident Dp -branes.

In the solutions (1) the lightcone coordinates scale *asymmetrically* under the dilations

$$z \rightarrow \xi z, \quad x^- \rightarrow \xi^{2-a} x^-, \quad x^+ \rightarrow \xi^a x^+, \quad \vec{x} \rightarrow \xi \vec{x} \quad (2)$$

with the dynamical exponent $a = \frac{2p-12}{p-5}$. Note, under this scaling the string coupling, e^ϕ , and the string metric in eq.(1) do get conformally rescaled (for $p \neq 3$). Thus for $p \neq 3$ the scaling (2) is not a symmetry of the solutions. This is a well known RG property of the Dp -brane AdS vacuas; see eq. (45) in the Appendix. Upon lightcone compactification, various conformal factors in the metric (1) contribute to the overall hyperscaling (conformal scaling) property of the Lifshitz metric, see next eq.(3). Note that x^- spatial coordinate of the Dp -brane has a different scaling as compared to the remaining $(p-1)$ spatial coordinates x^i 's. The latter $p-1$ coordinates do have a rotational symmetry amongst them. We are mainly interested in the situation where x^- is taken a compact coordinate. Note it is the compactification of x^- that gives us a "conformally Lifshitz" metric in lower dimensions. Thus the solutions (1) have all that one would require for a hyperscaling Lifshitz spacetime description at the IR fixed point [10].

As emphasized above we shall have to take x^- being compact so as to get the actual Lifshitz like solutions. We write down explicit compactification of the solutions (1). Upon compactifications along the circle x^- , also along the sphere S^{8-p} , we get the $(p+1)$ -dimensional conformally Lifshitz metric (given in the Einstein frame)

$$ds_{lif_{p+1}}^2 \sim z^{\frac{2(p^2-6p+7)}{(p-1)(p-5)}} \left(-\frac{(dx^+)^2}{\beta^2 z^{2a_{lif}}} + \frac{d\vec{x}_{p-1}^2 + dz^2}{z^2} \right). \quad (3)$$

Note these Lifshitz metrics have a specific conformal factor, of the type $z^{\frac{2\theta}{p-1}}$, and the corresponding fact is summarized by defining a hyperscaling parameter θ

$$\theta_{lif} = \frac{p^2 - 6p + 7}{p - 5}, \quad (4)$$

which characterises these Lifshitz string solutions. Note that θ_{lif} is never vanishing for these conformally Lifshitz solutions (3). Actually these solutions essentially describe a nonrelativistic Lifshitz dynamics at the IR fixed point. This description is however valid over a limited holographic range only. For example, these solutions cannot be good solutions for UV description of a Lifshitz CFT, because in the UV region the size of x^- circle in the geometry would become sub-stringy. In other words the effective string coupling will diverge in the UV. Hence for these solutions to have a suitable UV description we have had to modify them and attach appropriate asymptotic AdS configuration, see [33, 8]. That program leads us to the interpolating class of Lifshitz vacua.

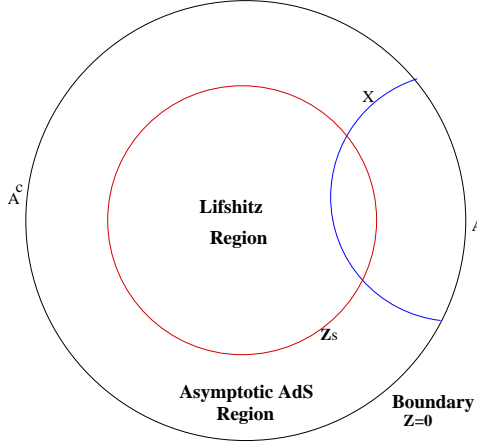


Figure 1: The central Lifshitz region ends at $z = z_s$ and smoothly connects to asymptotic AdS region.

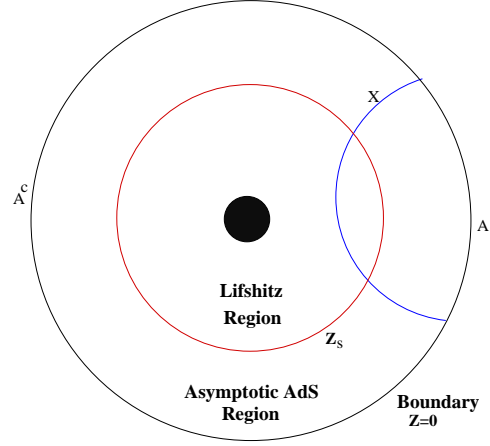


Figure 2: The Lifshitz-AdS spacetime with a black hole at the center. Any minimal surface X can reach only upto the horizon.

The interpolating Lifshitz-AdS solutions can be written as (for $p \neq 5$) [33]

$$\begin{aligned}
 ds_{Lif-AdS}^2 &= R_p^2 z^{\frac{p-3}{p-5}} \left[\left\{ \frac{K}{z^2} (dx^-)^2 + \frac{-dx^+ dx^- + d\vec{x}_{(p-1)}^2}{z^2} + \frac{4}{(5-p)^2} \frac{dz^2}{z^2} \right\} + d\Omega_{(8-p)}^2 \right] \\
 e^\phi &= (2\pi)^{2-p} g_{YM}^2 R_p^{3-p} z^{\frac{(7-p)(p-3)}{2p-10}}
 \end{aligned} \tag{5}$$

with the same $(p+2)$ -form flux. The new function

$$K(z) = v + \left(\frac{z}{z_{IR}} \right)^{\frac{2p-14}{p-5}} \equiv v \left(1 + \left(\frac{z}{z_s} \right)^{\frac{2p-14}{p-5}} \right) \tag{6}$$

is a harmonic function and plays the role of an interpolating function. The parameter $z_{IR} > 0$ is an intermediate IR scale and is related to β given earlier. Note that the solution (5) is interpolating solution because now the metric (5) smoothly connects Lifshitz and asymptotic AdS regions, provided v is finite. Having finite v does imply a presence of a chemical potential in the CFT [33].² In the asymptotic region, $z \ll z_{IR}$, and there $K \approx v$, the solution (5) starts behaving like conformally AdS geometry ($a = 1$). While in the IR region $z \gg z_{IR}$, where $K \approx \left(\frac{z}{z_{IR}} \right)^{\frac{2(p-7)}{p-5}}$, it behaves like a Lifshitz spacetime. Note that, since these solutions are interpolating configurations the scaling properties of the metric (5) will not be explicit at the intermediate scales. The *scaling* property of the metric will become explicit only in the neighbourhood of the respective IR or UV fixed points. An explicit lightcone compactification of the interpolating solutions (5) provides following $(p+1)$ -dimensional Lifshitz spacetime (Einstein frame metric)

$$ds_{p+1}^2 = L^2 z^{\frac{2\theta_{rel}}{(p-1)}} K^{\frac{1}{p-1}} \left[-\frac{(dx^+)^2}{4z^2 K} + \frac{d\vec{x}_{(p-1)}^2}{z^2} + \frac{4}{(5-p)^2} \frac{dz^2}{z^2} \right] \tag{7}$$

²Note that in Ref.[33] we simply took $v = 1$.

where K is given above in (6). Additionally there is always a running $(p+1)$ -dimensional dilaton field

$$e^{-2\phi_{(p+1)}} \sim z^{\frac{p-5}{2}} \sqrt{K} \quad (8)$$

and a Kaluza-Klein gauge field

$$A_{(1)} = -\frac{1}{2K} dx^+, \quad (9)$$

and the flux component of RR-form. Note the $\theta_{rel} = \frac{p^2-7p+14}{p-5}$ in the above is the effective hyperscaling parameter in the asymptotic UV region. The parameter L is an specific size factor which directly follows from compactification. One can see that near $z \sim 0$, K becomes a constant and the metric becomes conformally AdS type, as it should be for the relativistic ($a = 1$) CFT. We must emphasize here, that these descriptions are valid so long as string coupling remains perturbative and the spacetime curvature remains small. Beyond these UV scales, we must lift our solutions to M-theory for valid holographic description, see for example [17].

Since these solutions interpolate between two asymptotia, the value of hyperscaling parameter θ will switch in between

$$\theta_{lif} \geq \theta \geq \theta_{rel} \quad (10)$$

and correspondingly the dynamical exponent will vary in between

$$a_{lif} \geq a \geq a_{rel}. \quad (11)$$

For the conformally AdS spacetime $a_{rel} = 1$ and $\theta_{rel} < 0$ [33].

Expanding the time component of the gauge field (9) in the neighborhood of the boundary ($z \sim 0$), we find (for $p = 2, 3, 4$)

$$A_+(z \sim 0) = -\frac{1}{2r^{-v}} \left(1 - \frac{1}{v} \left(\frac{z}{z_{IR}} \right)^{\frac{2p-14}{p-5}} + \dots \right). \quad (12)$$

Thus the chemical potential and the charge (number) density can be found to be

$$\mu = -\frac{1}{2r^{-v}}, \quad \rho = \frac{N}{V_{(p-1)}} \simeq \frac{(R_p)^{3p-6} (r^-)^2}{G_{p+2}} \left(\frac{1}{z_{IR}} \right)^{\frac{2p-14}{p-5}} \quad (13)$$

Here G_{p+2} is the Newton's constant in $(p+2)$ dimensions, and $V_{(p-1)}$ is the regulated spatial volume of the p -dimensional system. Note we should never directly set $v = 0$ in these expressions as these are defined for finite v only. Since the chemical potential is nonvanishing, the CFT has a finite energy density $E \sim \mu \cdot \rho$. We have dropped overall normalisation factors in the expressions in equation (13).

The figure (1) represents a Lifshitz-AdS geometry with a minimal hypersurface X suspended inside the bulk geometry, while the figure (2) depicts that there could be a black hole inside Lifshitz geometry in the nonextremal case. Using the Lifshitz metric (7) the entanglement entropy of the strip-like subsystem in the boundary can be obtained as [33]

$$S_{Ent} = \frac{V_{p-2} L^d}{2G_{p+1}} \int_{z_*}^{\infty} dz z^{\frac{9-p}{p-5}} \frac{2}{(5-p)} \frac{K}{\sqrt{v + \left(\frac{z}{z_{IR}}\right)^{\frac{2(p-7)}{p-5}} - C^2 z^{\frac{2(p-9)}{p-5}}}} \quad (14)$$

where C is an integration constant which depends on the turning point z_* of the given extremal surface. The extremality equation is

$$\frac{dx_1}{dz} = \frac{2}{5-p} \frac{C z^{\frac{p-9}{p-5}}}{\sqrt{v + \left(\frac{z}{z_{IR}}\right)^{\frac{2(p-7)}{p-5}} - C^2 z^{\frac{2(p-9)}{p-5}}}} \quad (15)$$

These are the same expressions as were obtained in [33] except that there we took $v = 1$. One should also refer to the noncompact AdS-plane wave study in [27]. Our expressions naturally match with them. But we discuss compactified situation and the parameter like v has got definite interpretation in the compactified (Lifshitz) case, as giving rise to finite chemical potential in the boundary CFT. We avoid further discussion here, also a very parallel calculation will appear in the next section.

3 Schrödinger vacua with a spacetime screen

The string solutions with Schrödinger symmetry group have been well described in the initial works [1, 2, 4]. Particularly Schrödinger solutions with dynamical exponent $a = 2$ could be constructed out of $AdS_5 \times S^5$, by employing a combination of null Melvin twist and pair of T-dualities, involving a fibered direction along S^5 [2]. These correspond to the irrelevant operator deformations in the boundary CFT, so those solutions assume relativistic configurations in the IR. We are here interested in the IR Schrödinger solutions constructed by taking the double limits of boosted ‘bubble AdS solutions’ in [10]. These are given by [10]

$$ds_{Sch}^2 = R_p^2 z^{\frac{p-3}{p-5}} \left[\left\{ -\frac{\beta^2}{z^{4/(p-5)}} (dx^+)^2 + \frac{-dx^+ dx^- + d\vec{x}_{(p-1)}^2}{z^2} + \frac{4}{(5-p)^2} \frac{dz^2}{z^2} \right\} + d\Omega_{(8-p)}^2 \right],$$

$$e^\phi = (2\pi)^{2-p} (g_{YM})^2 R_p^{3-p} z^{\frac{(7-p)(p-3)}{2(p-5)}} \quad (16)$$

with the $(p+2)$ -form RR flux ($p \neq 5$), being similar to the Lifshitz case. It can be noted that these Schrödinger vacua are related via Wick rotations (along lightcone coordinates

x^+, x^-) of the corresponding Lifshitz solutions [10]. One significant difference between (1) and (16) is that in the Lifshitz case it is the metric component g_{--} which is nontrivial and positive definite, while in the Schrödinger solutions it is g_{++} which is nontrivial and is a negative quantity. The other background fields such as the dilaton and the $(p+2)$ -form flux however remain the same in both type of nonrelativistic solutions. Actually this relationship is reminiscent of the known fact that the black D p -branes and the bubble D p -branes get mapped into each other under double Wick rotations too.

In the above Schrödinger solutions the lightcone coordinates scale *asymmetrically* in a specific manner, under the dilatations

$$z \rightarrow \xi z, \quad x^+ \rightarrow \xi^{\frac{2}{p-5}} x^+, \quad x^- \rightarrow \xi^{\frac{p-7}{p-5}} x^-, \quad \vec{x} \rightarrow \xi \vec{x}$$

while the dilaton field and the metric in eq.(16) conformally rescale as in eq. (45). Thus the dynamical exponent of time in Schrödinger solutions is [10]

$$a_{sch} = \frac{2}{p-5}$$

which is negative for $p < 5$. We shall be mainly interested in these cases only.

It is however very crucial to bear in mind that these Schrödinger vacua cannot be immediately compactified along the x^- direction, because x^- is actually a null coordinate, i.e. ($g_{--} = 0$). So the nonrelativistic interpretation of the boundary CFT remains the least understood concept for the Schrödinger solutions, because such classical bulk geometry (16) cannot be used for any useful calculations. Thus what should be our approach to have a meaningful nonrelativistic Schrödinger description. A remedy was suggested in [4] whereby one could include a black hole in the interior of the asymptotically (UV) Schrödinger vacua. But this led to a finite temperature CFT. Here instead we have got IR Schrödinger solutions. In this work we shall try to modify our IR solutions by adding appropriate asymptotic (UV) AdS configurations.

3.1 Schrödinger (spacetime) screen

We shall selectively modify the Schrödinger solutions (16) and attach asymptotic AdS configuration to these IR solutions. Thus we apply a ‘Galilian boost’ to the Schrödinger solutions along the spacial x^- coordinate,

$$x^- \rightarrow x^- - vx^+, \quad x^+ \rightarrow x^+ . \quad (17)$$

Here $v > 0$ is a boost parameter and is dimensionless. Taking $v < 0$ does not lead to any interesting situation. In the boosted coordinates the metric (16) assumes the following

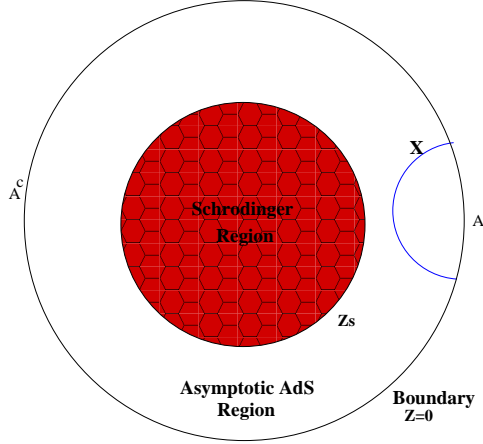


Figure 3: The Schrödinger screen is located at $z = z_s$. The central Schrödinger spacetime will not be accessible to an observer located in the asymptotic region ($z < z_s$). The central region would appear as a ‘halo’ to an outside observer.

form

$$\begin{aligned}
ds_{Sch-AdS}^2 &= R_p^2 z^{\frac{p-3}{p-5}} \left[\left(\frac{v}{z^2} - \frac{\beta^2}{z^{4/p-5}} \right) (dx^+)^2 + \frac{-dx^+ dx^- + d\vec{x}_{(p-1)}^2}{z^2} + \frac{4}{(5-p)^2} \frac{dz^2}{z^2} \right] + d\Omega_{(8-p)}^2 \\
&\equiv R_p^2 z^{\frac{p-3}{p-5}} \left[K_s \frac{(dx^+)^2}{z^2} + \frac{-dx^+ dx^- + d\vec{x}_{(p-1)}^2}{z^2} + \frac{4}{(5-p)^2} \frac{dz^2}{z^2} \right], \quad (18)
\end{aligned}$$

(Alternatively, one could directly obtain them following the boosted bubble solutions given in the Appendix.) While the dilaton and $(p+2)$ -form flux will remain unchanged. The new function K_s is given by

$$K_s = v - \left(\frac{z}{z_{IR}} \right)^{\frac{2p-14}{p-5}} \equiv v \left(1 - \left(\frac{z}{z_s} \right)^{\frac{2p-14}{p-5}} \right) \quad (19)$$

The various parameters are related as $\beta^2 = \frac{14-2p}{z_{IR}^{\frac{p-5}{p-5}}}$ and $v = (z_s/z_{IR})^{\frac{2p-14}{p-5}}$. Note that K_s vanishes for the special value $z = z_s$ and will flip its sign across this point. Due to this the two light-cone coordinates x^+, x^- will exchange their respective space and time nature across $z = z_s$. Thus, in the asymptotic region ($0 < z < z_s$), where x^+ will behave as spacelike direction with x^- being the time, while in the interior Schrödinger region ($z > z_s$) their roles would get reversed. This is somewhat reminiscent of the situation we encounter at the horizon of a black hole. But, the $z = z_s$ surface is a cool frontier, as there is no real singularity hidden inside the Schrödinger region. The curvature scalar remains smooth every where. In order to check this, we take the case of D3-brane, for which dilaton is constant and the string metric becomes

$$R^2 \left\{ \left(\frac{v}{z^2} - \beta^2 z^2 \right) (dx^+)^2 + \frac{-dx^+ dx^- + d\vec{x}_{(2)}^2}{z^2} + \frac{dz^2}{z^2} \right\} + R^2 d\Omega_{(5)}^2$$

which is a constant curvature spacetime. Note that the determinant of the string metric is independent of K_s . Thus in these new coordinates there is a kind of **screen** located at $z = z_s$, which an outside (AdS) observer will always encounter whenever it crosses the screen. Here onwards we shall refer the $z = z_s$ hypersurface, which is topologically $R^{1,p} \times S^{8-p}$, simply as a **Schrödinger spacetime screen** in order to distinguish it from a black hole horizon. The interior of Schrödinger screen will always include a Schrödinger spacetime. The interior spacetime would appear as a ‘halo’ from the outside of the screen; see the sketch in figure (3).³ Ultimately, we think that this situation leads to a *reduction in the entanglement entropy* as we find next. The main reason for this reduction is that the interior side of the screen remains inaccessible to the outside observers. Correspondingly in the boundary CFT some states would be ‘disentangled’.⁴

3.2 Lightcone compactification and IR singularity

We discussed above that Schrödinger screen is a smooth surface where the two lightcone coordinates exchange their spacetime nature. Especially in the asymptotic AdS region, $0 < z < z_s$, where x^+ behaves as a spatial coordinate, we could think of compactifying x^+ on a circle; $x^+ \sim x^+ + 2\pi r^+$. The compactified solution, which is good in the asymptotic region only, will be given by (in Einstein frame metric)

$$ds_{p+1}^2 = L^2 z^{\frac{2(p^2-7p+14)}{(p-1)(p-5)}} K_s^{\frac{1}{p-1}} \left[-\frac{(dx^-)^2}{4z^2 K_s} + \frac{d\vec{x}_{(p-1)}^2}{z^2} + \frac{4}{(5-p)^2} \frac{dz^2}{z^2} \right] \quad (20)$$

where x^- is to be treated as being the time coordinate. There is a running dilaton field and the Kaluza-Klein gauge field

$$\begin{aligned} e^{2\phi_{p+1}} &\sim \frac{z^{\frac{5-p}{2}}}{\sqrt{K_s}} \\ A_{(1)} &\sim -\frac{1}{2K_s} dx^- \end{aligned} \quad (21)$$

Note $K_s = v - \left(\frac{z}{z_{IR}}\right)^{\frac{2p-14}{p-5}}$, is positive definite outside the Schrödinger region. Thus the $(p+1)$ -dimensional metric (20) remains faithful only outside of the Schrödinger screen.

It is important to note that in the lightcone compactified solutions (20), we have unwittingly introduced an essential singularity at $z = z_s$, because this lightcone circle is shrinkable at $z = z_s$. Thus the compactified description holds good in the $z < z_s$ region

³Note that there is no obstruction for an observer in crossing the screen, only thing it has to do after crossing the screen is that it has to readjust its coordinates (x^+, x^-). The z remains a valid holographic coordinate across $z = z_s$. The spacetime is geodesically complete in this sense. But an static observer located in the $z < z_s$ cannot communicate with its counterpart situated in $z > z_s$ region.

⁴ This might appear analogous to the screening effects in condensed matter systems, perhaps due to some concentration of hidden negatively charged (hole) states.

only and it breaks down near $z = z_s$.⁵ Back in ten dimensions we already know that the ‘noncompact’ solutions are smooth at $z = z_s$. The singularity gets introduced in an artificial way only, when we employ the compactification. In the light of this discussion we conclude that whatever conclusions we draw in the rest of the paper will only be good for an effective description valid over a limited UV regime $z < z_s$.

3.3 Confinement in the IR region

As we learned above, upon lightcone compactification the $(p + 1)$ -dimensional effective string coupling in (21), $\langle e^{\phi_{p+1}} \rangle$, becomes stronger near $z = z_s$ much faster than the usual (relativistic) RG flow. In fact it becomes singular, so we cannot trust the lower dimensional interpretation very close to $z = z_s$. It would be appropriate that as we approach $z = z_s$ we should ideally up-lift the solution (20) back to 10-dimensions and consider stringy coorections.

The presence of the KK fields in (21) implies a presence of finite chemical potential, and following from eq.(13) we can determine

$$\mu \sim -\frac{1}{2r^{+\nu}}$$

in the p -dimensional Schrödinger CFT near the UV fixed point, associated with an effective (negative) charge density

$$\rho \sim -\frac{(R_p)^{3p-6}(r^+)^2}{G_{p+2}} \left(\frac{1}{z_{IR}} \right)^{\frac{2p-14}{p-5}}.$$

Only change is in the sign of the charge density from the expressions given in (13) for the Lifshitz backgrounds. Thus these quantities make the defining characteristics of the boundary Schrödinger CFT near the UV fixed point. It means that such a Galilean Yang-Mills theory would flow towards the IR region where its effective gauge coupling becomes stronger near an intermediate scale $z = z_s$ and the bulk geometry would ultimately encounter a Schrödinger screen. Some of these are the known characteristics of confining YM theories, more like confinement in QCD. (For example, we could consider N D4-branes with Schrödinger IR deformation so that the corresponding boundary theory is

⁵ We would like to note that it is the usual situation whenever compactification involves a shrinkable circle. Hence we should either remove or resolve this singularity. The simple way of handling the substringy circle size in our solutions would be to lift the solution back to ten dimensions. In 10D, we may include higher order corrections to the string solutions near z_s , which could cloak the singularity. But this study is beyond the scope of this paper. However, when viewed from 10D the compact lightcone coordinate starts becoming null as $z \rightarrow z_s$. Eventhough this 10D geometry cannot be trusted near z_s , but DLCQ description might eventually hold good there; see [4] for DLCQ of null lightcone compactification. Alternatively, one can do a T-duality along the compact circle as well.

4D Schrödinger CFT, i.e. a lightcone compactified 5D SYM with suitable operator deformations related to chemical potential and (negative) charge density as described above.) The generic analysis based on Schrödinger-AdS bulk spacetime predicts a confinement in $D \leq 4$ for a Schrödinger CFT at some intermediate IR scale z_s .

3.4 Entanglement Entropy in Schrödinger-AdS systems

In order to find the entanglement entropy (EE) of a subsystem of a Schrödinger CFT, we will use the interpolating solution (20), only for simplicity.⁶ Thus we pick up a subsystem A (with its boundary ∂A) in the CFT. The subsystem A will naturally have an entanglement of its states with its complement A^c , which supposedly is comparatively larger system. The entanglement entropy of the subsystem A is described geometrically (holographically) in terms of the area of an extremal surface $X_{(p-1)}$ (spacelike $(p-1)$ -dimensional surface) ending on the boundary ∂A , see [30]. Thus we have for entanglement entropy

$$S_{Ent}(A) = \frac{1}{4G_{p+1}} [Area]_X \quad (22)$$

The extremal surface $X_{(p-1)}$ lies within the bulk spacetime, which is a $(p+1)$ -dimensional Schrödinger spacetime being asymptotically conformally AdS_{p+1} . We pick up the subsystem A such that it is a rectangular strip with width along $x^1(z)$ and stretched along rest of x^i 's, at any fixed time. (Note we have taken x^+ being a compact coordinate.) Also, x^- is being identified with boundary time coordinate. The range of x_1 coordinate is $-l/2 \leq x_1 \leq l/2$ and the regulated (but large) size of other coordinates is $0 \leq x^i \leq l^i$ ($l^i \gg l$) for $i = 2, \dots, p-1$. Considering the $(p+1)$ -dimensional Einstein metric (20), we find

$$S_{Ent} = \frac{V_{p-2} L^d}{2G_{p+1}} \int_{z_*}^{z_\infty} dz z^{\frac{9-p}{p-5}} \sqrt{K_s} \sqrt{\frac{4}{(5-p)^2} + (x'_1)^2} \quad (23)$$

where $z_\infty \approx 0$ is the UV cut-off and z_* is the turning point. $V_{p-2} = l_2 \cdots l_{p-1}$ is the volume of the ensemble box stretched along the spatial directions x_2, \dots, x_{p-1} . K_s is as given in (19). From (23) we determine that the minimal surface satisfies the first order equation

$$\begin{aligned} \frac{dx_1}{dz} &= \frac{2}{5-p} \frac{C z^{\frac{p-9}{p-5}}}{\sqrt{v - \left(\frac{z}{z_{IR}}\right)^{\frac{2(p-7)}{p-5}} - C^2 z^{\frac{2(p-9)}{p-5}}}} \\ &\equiv \frac{2}{5-p} \frac{\left(\frac{z}{z_c}\right)^{\frac{p-9}{p-5}}}{\sqrt{1 - \left(\frac{z}{z_s}\right)^{\frac{2(p-7)}{p-5}} - \left(\frac{z}{z_c}\right)^{\frac{2(p-9)}{p-5}}}} \end{aligned}$$

⁶ Note, the entanglement entropy can also be obtained by using the 10D metric where lightcone coordinate is not compactified. The basic expression remains unchanged for a strip-like subsystem except minor changes in the Newton's constant and volume like parameters.

(24)

where C is an integration constant and we redefined $\frac{C^2}{v} = \left(\frac{1}{z_c}\right)^{\frac{2(p-9)}{p-5}}$. At the turning point

$$1 - \left(\frac{z}{z_s}\right)^{\frac{2(p-7)}{p-5}} - \left(\frac{z}{z_c}\right)^{\frac{2(p-9)}{p-5}} = 0 \quad (25)$$

where $x'_1|_{z_*} = \infty$ and $x_1(z_*) = 0$. While at the boundary points $x'_1|_{z=0} \sim 0$, where boundary condition is $x_1(0) = l/2$.

Finding solutions of the first order differential equation (24) is much like solving a classical orbit in the central force problem with the given initial conditions. The term $C^2 z^{\frac{2(p-9)}{p-5}}$ plays the role of a repulsive ‘centrifugal type potential’, while the term $\left(\frac{z}{z_{IR}}\right)^{\frac{2(p-7)}{p-5}}$ behaves like a *repulsive* central potential. It is easy to see that the latter repulsive force arises due to the interior Schrödinger region which repels the classical trajectories approaching from the boundary with certain fixed energy $E \equiv E(v)$. Higher is the v the higher will be the penetrating power of the projectile, which ultimately has to bounce back. In any case these orbits can never penetrate the central potential barrier. The point of closest approach, z_* , will be restricted to being $z_* > z_s$. Thus the IR Schrödinger spacetime leads to a central repulsive force, while the universal component of repulsive force comes from the curvature of AdS spacetime. Note that this situation is different to that of the Lifshitz solutions discussed in the last section, where there existed an ‘attractive’ component in the effective potential, see [33].

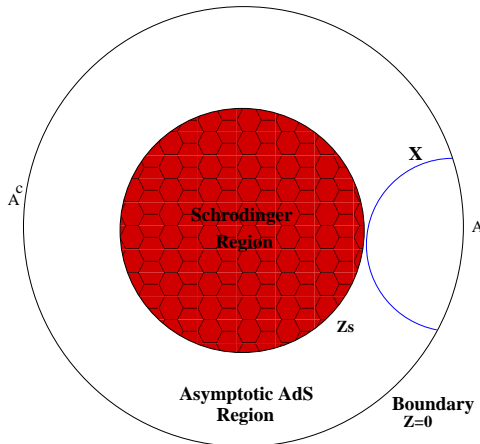


Figure 4: A large extremal surface X will glance the Schrödinger screen but at the safe distance $z_* < z_s$.

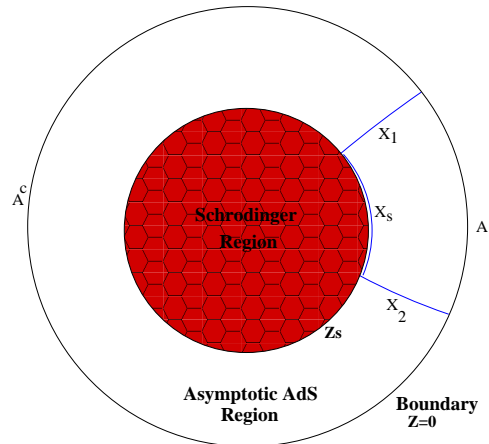


Figure 5: Eventually as the size of the boundary subsystem increases, the extremal surface has three parts X_1 , X_s , and X_2 . The X_s part glances the Schrödinger screen from a safe location $z = z_*$.

We shall be interested in the situation where $z_s \gg z_c$. It can be inferred that in the Schrödinger case the turning point will always arise in the region $z < z_c$ and in this region

the geometry (20) is well defined. While in the Lifshitz case, due to attractive component in the potential the turning point arises for $z > z_c$. So keeping everything else the same, the Lifshitz orbits are generally longer in depth. This gives an entanglement entropy formula for the Schrödinger system as

$$S_{Ent} = \frac{V_{p-2}L^d}{2G_{p+1}} \frac{2\sqrt{v}}{(5-p)} \int_{z_*}^{z_\infty} dz z^{\frac{9-p}{p-5}} \frac{1 - \left(\frac{z}{z_s}\right)^{\frac{2(p-7)}{p-5}}}{\sqrt{1 - \left(\frac{z}{z_s}\right)^{\frac{2(p-7)}{p-5}} - \left(\frac{z}{z_c}\right)^{\frac{2(p-9)}{p-5}}} \quad (26)$$

If we set $z_s = \infty$, the expression (26) reduces to the entanglement entropy in the relativistic CFT system. The turning point of the extremal surface in the conformally AdS case appears at the value $z = z_c$. While we will always get $z_* < z_c$ for the Schrödinger-AdS system due to repulsive nature of the potential. Thus the area of the extremal surface X is going to be smaller for the Schrödinger-AdS spacetime compared to the purely conformally AdS case. While we already know that the area of the extremal surface has been larger in the Lifshitz-AdS case as compared to the pure conformally AdS case [33]. Thus we can establish the hierarchy of the entanglement entropies,

$$S_{Ent}^{Lif-AdS} > S_{Ent}^{AdS} > S_{Ent}^{Sch-AdS}. \quad (27)$$

provided the global system parameters, like v , the size l (or z_*) and z_{IR} are kept the same.

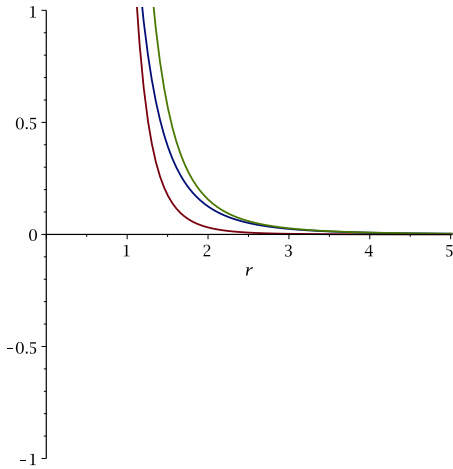


Figure 6: A plot of various components of the effective (Schrödinger-AdS) potential V_{eff} (for $p = 3$). The green color (right most) curve gives the resulting potential which is repulsive.

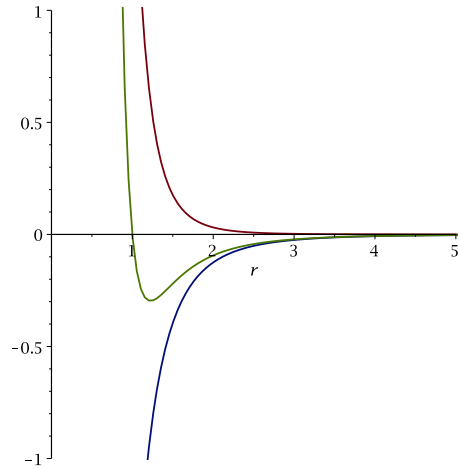


Figure 7: A plot of the various components of the Lifshitz-AdS potential V_{eff} , for $p = 3$. The green color (middle curve) gives the resultant potential which is attractive in the asymptotic regime.

3.5 A troika of the solutions

The analysis of the previous sections provides us with a general entanglement entropy formula for the Schrödinger-AdS, conformally AdS and Lifshitz-AdS bulk solutions

$$S_{Ent} = \frac{V_{p-2}L^d}{2G_{p+1}} \frac{2}{(5-p)} \int_{z_*}^{z_\infty} dz z^{\frac{9-p}{p-5}} \frac{K(z)}{\sqrt{v - V_{eff}}}. \quad (28)$$

The effective potential appearing in the three cases can be classified as

$$\begin{aligned} V_{eff} &= -\left(\frac{z}{z_{IR}}\right)^{\frac{2(p-7)}{p-5}} + C^2 z^{\frac{2(p-9)}{p-5}} && \text{Lifshitz - AdS} \\ &= \left(\frac{z}{z_{IR}}\right)^{\frac{2(p-7)}{p-5}} + C^2 z^{\frac{2(p-9)}{p-5}} && \text{Schrodinger - AdS} \\ &= C^2 z^{\frac{2(p-9)}{p-5}} && \text{conformally AdS} \end{aligned} \quad (29)$$

while the numerator in the integrand will read as

$$\begin{aligned} K(z) &= v + \left(\frac{z}{z_{IR}}\right)^{\frac{2(p-7)}{p-5}} && \text{Lifshitz - AdS} \\ &= v - \left(\frac{z}{z_{IR}}\right)^{\frac{2(p-7)}{p-5}} && \text{Schrodinger - AdS} \\ &= v && \text{conformally AdS} \end{aligned} \quad (30)$$

Especially for $p = 3$ case the effective potential is plotted for some arbitrary but fixed values of the parameters in the figure (6) for Schrödinger-AdS, and in figure (7) for the Lifshitz-AdS solutions. Note that we have also redefined the holographic coordinate back to $r = z^{\frac{2}{p-5}}$ for the convenience in these plots, so that

$$\begin{aligned} V_{eff} &= -\left(\frac{r_{IR}}{r}\right)^{7-p} + \frac{C^2}{r^{9-p}} && \text{Lifshitz - AdS} \\ &= \left(\frac{r_{IR}}{r}\right)^{7-p} + \frac{C^2}{r^{9-p}} && \text{Schrodinger - AdS} \\ &= \frac{C^2}{r^{9-p}} && \text{conformally AdS} \end{aligned} \quad (31)$$

4 Numerical analysis

Although we have qualitatively understood the holographic picture of the Schrödinger-AdS bulk solutions, it would be worth while to make it concrete with some numerical calculations. For this purpose we pick up an special case of D3-brane. We rewrite the integral equation governing the extremal (entanglement) surface as

$$x_1(b) = r_*^3 \sqrt{K_*} \int_{r_*}^b dr \frac{r^{-5}}{\sqrt{1 - \frac{r_*^4}{r^4} - \frac{r_*^6 K_*}{r^6}}} \quad (32)$$

note that $x_1(r_*) = 0$. We have taken $K(r) = 1 - \frac{r^4}{r_*^4}$ and in our notation $K_* \equiv K(r)|_{r=r_*}$. Actually the parameter b representing the boundary value of holographic coordinate should be taken reasonably large so as to represent boundary location. Similarly the entanglement entropy integral can be expressed as

$$S(b) = S_0 \sqrt{v} \int_{r_*}^b dr \frac{r^{-1} K(r)}{\sqrt{1 - \frac{r^4}{r_*^4} - \frac{r_*^6 K_*}{r^6}}} \quad (33)$$

where $S_0 \equiv \frac{V_1 L^2}{2G_4}$ is an overall constant in the entropy expression. We will set $S_0 = 1$ in rest of the analysis. In our strategy we consider a small (perturbative) value of $r_s = .1$ and set $v = 100$. Note that turning point of the extremal surface for Schrödinger-AdS solutions always arise outside of the screen, that is $r_* > r_s$. For various values of these turning points, $r_* > r_s$, we numerically evaluate above first integrals. The graphs for $x_1(b)$ vs b have been plotted in figure (8) over sufficiently large range of b . We have selectively taken $r_* = .12, .15, .2$ and $.5$. In fact one could take any other set of allowed values. We observe that $x_1(b)$ graphs become flatter at large b , which gives the idea of system size. Recall that typically the asymptotic value $x_1(\infty)$ gives us the system size, l , or the boundary value. Also we observe as the turning point r_* becomes deeper and deeper the subsystem size in the boundary CFT increases. This is an expected behaviour. *The subsystem size will be largest for the trajectory which passes by near most to the Schrödinger screen at $r = r_s$.* We note that, as the size of system A increases, a part of extremal surface, X_s , would start glancing the Schrödinger screen from a fixed location $r = r_*$, see the figure (5). Note however these trajectories can never touch the screen located at $r = r_s$. The entanglement entropy contribution from X_s part of the surface, namely the part parallel to the Schrödinger screen, would however come out to be vanishingly small, due to $K^{\frac{1}{p-1}}$ factor in the metric. This implies that there is a limit to the entanglement entropy. Thus after a point, even if the subsystem size l increases, the entropy would stop increasing any further. Hence there is a saturation point in the Schrödinger-AdS system. We note down some of the values of entanglement entropy (for which we have safely taken UV cut-off to be $b = 1.5$)

$$S_{r_*=.12}^{Sch} = 11.1817, \quad S_{r_*=.15}^{Sch} = 11.1784, \quad S_{r_*=.2}^{Sch} = 11.1509, \quad S_{r_*=.5}^{Sch} = 10.705, \quad (34)$$

Thus we have

$$S_{r_*=.12}^{Sch} > S_{r_*=.15}^{Sch} > S_{r_*=.2}^{Sch} > S_{r_*=.5}^{Sch} \quad (35)$$

which means that the entanglement entropy increases alongwith the subsystem size. But as the extremal surfaces get closer to the Schrödinger screen, the entropy of the systems stops increasing with the system size. For example, for the extremal surfaces with $r_* = .12$ and $r_* = .15$ there is no appreciable change in the entanglement entropy. *We conclude that the part of the extremal surface, X_s , parallel to the Schrödinger screen has negligible*

contribution to the entanglement entropy. That is, correspondingly some states in the CFT would have negligible contribution to the entanglement or will remain hidden. Thus the Schrödinger screen leads to *reduced entanglement* in Schrödinger like solutions embedded in an asymptotically (conformally) AdS spacetimes.

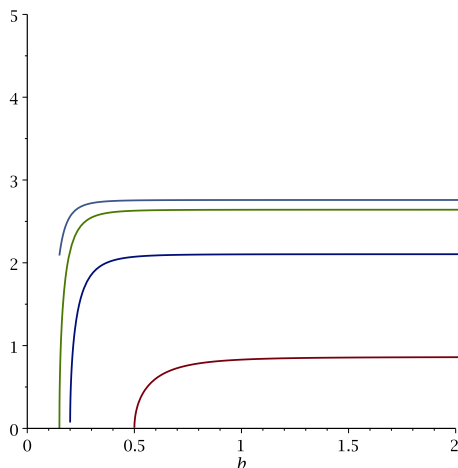


Figure 8: *Plots of the extremal trajectories, $x_1(b)$ for the Schrödinger CFT for the turning points $r_* = .12, .15, .2$ and $.5$. It shows that closer is the turning point to $r_s = .1$ (the Schrödinger screen) the larger is its impact parameter (or the size of the boundary CFT subsystem).*

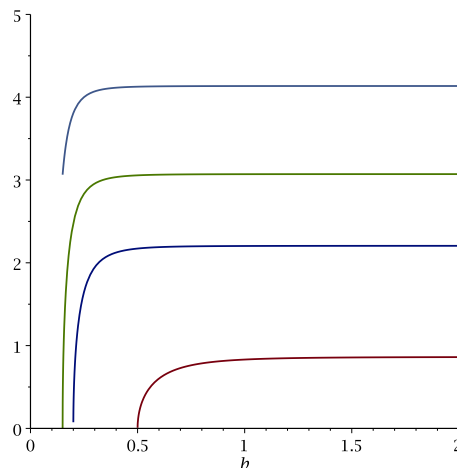


Figure 9: *Plots of the extremal trajectories $x_1(b)$ for the Lifshitz CFT for the turning point values $r_* = .12, .15, .2$ and $.5$. It shows that smaller the value of r_* larger is the impact parameter (or size of the boundary subsystem).*

This is altogether very different situation when compared with the Lifshitz-AdS cases. The first major difference in the two solutions is that the Lifshitz solutions do not have a screen (but they can include a black hole horizon). So, in principle, a large extremal surface can have a turning point situated well inside the Lifshitz (IR) region. For the purpose of the comparison, we have taken the same values of the turning points as in the Schrödinger case above. The graphs for $x_1(b)$ vs b have been plotted in figure (9) for the Lifshitz-AdS case. We have selectively taken $r_* = .12, .15, .2$ and $.5$. As expected orbits are large in the Lifshitz-AdS case. We do also find the entanglement entropy (with the same value $b = 1.5$ and other parameters being the same)

$$S_{r_*=.12}^{Lif} = 11.253, \quad S_{r_*=.15}^{Lif} = 11.224, \quad S_{r_*=.2}^{Lif} = 11.176, \quad S_{r_*=.5}^{Lif} = 10.709, \quad (36)$$

From the eqs. (34) and (36) we conclude that in general

$$S^{Lif-AdS} > S^{AdS} > S^{Sch-AdS}. \quad (37)$$

5 Conclusion

We have studied the Schrödinger type nonrelativistic Dp -brane solutions having conformally AdS asymptotic geometries. These specially engineered Schrödinger-AdS solutions possess a smooth ‘horizon’ like hypersurface, more appropriately a screen (or a mask), across which lightcone coordinates (x^-, x^+) flip their respective space and time nature. We only discussed zero temperature solutions. As we know a black hole horizon behaves like a finite temperature frontier and whose area gives black hole entropy. So in this sense the *Schrödinger screen* is totally different from the Schwarzschild horizon. For the Schrödinger-AdS solutions, an observer situated in the asymptotic AdS region will find the interior Schrödinger region to be completely inaccessible. *Thus some information will get hidden behind the Schrödinger screen.*

The presence of asymptotically AdS region in the Schrödinger solutions requires us to include finite chemical potential and a (negative) charge density. We have estimated the entanglement entropy of the strip-like subsystem in the boundary. It is found that the masked Schrödinger region does not contribute to the entanglement and this results in a net reduction of the entanglement entropy. The net effect of the Schrödinger screen is that it divides the spacetime into two isolated parts and this results in a loss of quantum information. This may indicate that a finite concentration of the negatively charged fermions, perhaps a finite concentration of the hole states (or vacancies in the fermi surface) could reduce the entanglement. We have worked in the regime where the charge density is much smaller (a perturbative regime) than the finite effect of chemical potential in the CFT. We do find that as the subsystem size increases the entanglement entropy initially increases along with the system size but it does not increase beyond a point and gets saturated. On the physical grounds this might be due to the fact that screening effects of the Schrödinger screen come into play. It requires to further investigate these kind of solutions and also identify analogous quantum phenomenon in condensed matter physics or fluid systems.

Acknowledgements: The author is an Associate of the ICTP, Trieste and acknowledges the generous support from the centre, where this work has come to the completion.

A The Dp -branes and the hyperscaling

The maximally supersymmetric near horizon AdS solutions are given by [17]

$$\begin{aligned}
 ds_{AdS}^2 &= R_p^2 r^{\frac{p-3}{2}} \left[r^{5-p} \{-dx^+ dx^- + d\vec{x}_{(p-1)}^2\} + \frac{dr^2}{r^2} + d\Omega_{(8-p)}^2 \right], \\
 e^\phi &= (2\pi)^{2-p} g_{YM}^2 R_p^{3-p} r^{\frac{(7-p)(p-3)}{4}}
 \end{aligned}
 \tag{38}$$

along with a suitable $(p + 2)$ -form field strength

$$F_{p+2} = (7 - p)R_p^{2p-2}r^{6-p}dr \wedge dx^+ \wedge dx^- \wedge [dx_{(p-1)}] \quad (39)$$

for the electric type Dp -branes ($p < 3$) and a $(8 - p)$ -form

$$F_{8-p} = (7 - p)R_p^4\omega_{8-p} \quad (40)$$

for the magnetic type (Hodge dual) Dp -branes ($p > 3$). Specially for D3-brane case we have $F_5 = 4(1 + \star)\omega_5$, which is self-dual 5-form field strength. We have introduced x^+, x^- as lightcone coordinates along the world volume of the branes, and $\vec{x}_{(p-1)}$ represents other $(p-1)$ spatial directions parallel to the Dp -brane, and as usual r is the radial (holographic) coordinate. The interpretation of various parameters can be found in [17] and also given in [8].

As emphasized in [33], in the above conformally $AdS_{p+2} \times S^{8-p}$ solutions, we could have taken slightly modified AdS line element

$$ds_{AdS}^2 = R_p^2 r^{\frac{p-3}{2}} \left[r^{5-p} [v(dx^-)^2 - dx^+ dx^- + d\vec{x}_{(p-1)}^2] + \frac{dr^2}{r^2} + d\Omega_{(8-p)}^2 \right], \quad (41)$$

Namely we have introduced a constant $g_{--} > 0$ component, but note that $v > 0$. Doing this is actually harmless as it still remains an AdS vacua. (The reason is that the constant g_{--} term can be reabsorbed by a coordinate shift, like $x^+ \rightarrow x^+ + vx^-$, if and when the need arises.) However, certain global symmetries of the metric, such as the lightcone boost $x^- \rightarrow \lambda x^-$, $x^+ \rightarrow \frac{1}{\lambda} x^+$, may not be manifest in the shifted coordinate frame. The inclusion of constant g_{--} component in these solutions is useful in the following way. We shall be considering (nonrelativistic) Schroedinger-like solutions which have nontrivial g_{++} deformations. Since Schrödinger solutions have $g_{++} < 0$, so x^+ is a timelike coordinate in them. Once we employ the above constant shift in these Schrodinger solutions then in some spacetime region we will find x^+ to behave like a space like coordinate, i.e. $g_{++} \geq 0$. In this region we can also make it a compact direction and the subsequent DLCQ description of the holographic theory would then follow. Not that we need large discrete momentum modes in the compact direction as it is this sector which tends to behave nonrelativistically.

Let us redefine the radial coordinate

$$r^{p-5} = z^2 \quad \text{for } p \neq 5 \quad (42)$$

With z as holographic coordinate and some scaling of the brane coordinates the above solutions can be brought to the form

$$ds^2 = R_p^2 z^{\frac{p-3}{p-5}} \left[\left\{ \frac{v(dx^+)^2}{z^2} + \frac{-dx^+ dx^- + d\vec{x}_{(p-1)}^2}{z^2} + \frac{4}{(5-p)^2} \frac{dz^2}{z^2} \right\} + d\Omega_{(8-p)}^2 \right]$$

$$e^\phi = (2\pi)^{2-p} g_{YM}^2 R_p^{3-p} z^{\frac{(7-p)(p-3)}{2(p-5)}} \quad (43)$$

along with the $(p + 2)$ -form flux. One can find that under the dilatations $z \rightarrow \xi z$, the brane coordinates would rescale as

$$x^\pm \rightarrow \xi x^\pm, \quad \vec{x} \rightarrow \xi \vec{x} \quad (44)$$

while the dilaton and the string metric in (43) conformally rescale as

$$g_{MN} \rightarrow \xi^{\frac{p-3}{p-5}} g_{MN}, \quad e^\phi \rightarrow \xi^{\frac{(7-p)(p-3)}{2(p-5)}} e^\phi \quad (45)$$

Note this overall conformal rescaling is the standard Weyl rescaling behaviour, of conformally AdS solutions [17], giving rise to the RG flow in the boundary CFT. From Eq.(44) the dynamical exponent of time is $a \equiv a_{rel} = 1$, so that the boundary theories are $(p + 1)$ -dimensional ‘relativistic’ CFT $_{(p+1)}$ with sixteen supercharges. Note, once x^+ is taken to be a coordinate on a circle, the boundary CFT becomes a DLCQ theory and is a p -dimensional theory. While the compactification of the bulk solution (43) along x^- and S^{8-p} , results in $(p + 1)$ -dimensional (Einstein) metric given as

$$\begin{aligned} ds_{p+1}^2 &\sim z^{\left(\frac{p-5}{p-1} + \frac{p-3}{p-5}\right)} \left[-\frac{(dx^+)^2}{z^2} + \frac{d\vec{x}_{(p-1)}^2}{z^2} + \frac{4}{(5-p)^2} \frac{dz^2}{z^2} \right] \\ &= z^{\frac{2(p^2-7p+14)}{(p-1)(p-5)}} \left[-\frac{(dx^+)^2}{z^2} + \frac{d\vec{x}_{(p-1)}^2}{z^2} + \frac{4}{(5-p)^2} \frac{dz^2}{z^2} \right] \equiv z^{\frac{2\theta}{d}} ds_{AdS_{p+1}}^2. \end{aligned} \quad (46)$$

From where we can read the hyperscaling parameter to be

$$\theta = \frac{p^2 - 7p + 14}{p - 5} \equiv \theta_{rel}. \quad (47)$$

Note that, $d \equiv p - 1$ gives the total number of spatial directions of the boundary CFT $_p$. Let us mention here that there is also a running $(p + 1)$ -dimensional dilaton field

$$e^{-2\phi_{(p+1)}} \sim z^{\frac{p-5}{2}} \quad (48)$$

as well as fields arising out of the reduction of $(p + 2)$ -form RR field strength. These solutions are extremal solutions.

B Boosted Bubble solutions

We do note down the boosted bubble solutions for the sake of completeness. The procedure is the same as described in [10]. We take a AdS-bubble solution, make a shift of the spatial lightcone coordinate, and then Lorentz boost the system. The resultant solution is,

$$ds_{Bubble}^2 = R_p^2 z^{\frac{p-3}{p-5}} \left[\left\{ -\frac{g(dx^+)^2}{4z^2 K} + \frac{d\vec{x}_{(p-1)}^2}{z^2} + \frac{4}{(5-p)^2} \frac{dz^2}{gz^2} \right\} + \frac{K}{z^2} (dx^- - A)^2 + d\Omega_{(8-p)}^2 \right] \quad (49)$$

where 1-form

$$A \equiv \frac{(1+g) - v\lambda^{-2}(1-g)}{4K} dx^+$$

and the harmonic functions

$$\begin{aligned} g(z) &= 1 - \left(\frac{z}{z_0}\right)^{\frac{2p-14}{p-5}} \\ K(z) &= v - \frac{(v\lambda^{-1} + \lambda)^2}{4} \left(\frac{z}{z_0}\right)^{\frac{2p-14}{p-5}} \equiv v - \frac{1}{4} \left(\frac{z}{z_{IR}}\right)^{\frac{2p-14}{p-5}}. \end{aligned} \quad (50)$$

The dilaton and the $(p+2)$ -form field strength remain as in the AdS-bubble case. The bubble solutions are the nonextremal examples. These are smooth boosted bubble p -brane solutions and the holographic coordinate range is given as $z_0 \geq z \geq 0$. If $v \neq 0$, they become asymptotically conformally AdS solutions. The double limits $1/z_0 \rightarrow 0$, $\lambda \rightarrow \infty$, keeping $z_{IR} =$ fixed, will give us Schrödinger-AdS solutions (18), which are extremal cases.

References

- [1] D.T. Son, Phys. Rev. **D78** (2008) 046003, [arXiv:0804.3972[hep-th]].
- [2] K. Balasubramanian and J. McGreevy, Phys. Rev. Lett. **101** (2008) 061601, [arXiv:0804.4053[hep-th]]; K. Balasubramanian and J. McGreevy, JHEP 01 (2001) 137, [arXiv:1007.2184[hep-th]].
- [3] S. Kachru, X. Liu and M. Mulligan, "Gravity duals of Lifshitz-like Fixed Points", Phys. Rev. **D78** (2008) 106005, [arXiv:0808.1725[hep-th]].
- [4] J. Maldacena, D. Martelli and Y. Tachikawa, JHEP 0810 (2008) 072, arXiv:0807.1100.
- [5] K. Balasubramanian and K. Narayan, JHEP **1008**, 014 (2010), [arXiv:1005.3291[hep-th]].
- [6] H. Singh, "Special limits and non-relativistic solutions," JHEP **1012**, 061 (2010) [arXiv:1009.0651 [hep-th]].
- [7] R. Gregory, S. L. Parameswaran, G. Tasinato and I. Zavala, "Lifshitz solutions in supergravity and string theory," JHEP **1012** (2010) 047, [arXiv:1009.3445 [hep-th]].
- [8] H. Singh, "Holographic flows to IR Lifshitz spacetimes," JHEP **1104**, 118 (2011) [arXiv:1011.6221 [hep-th]].
- [9] G. Bertoldi, B. A. Burrington, A. W. Peet and I. G. Zadeh, "Lifshitz-like black brane thermodynamics in higher dimensions," Phys. Rev. D **83**, 126006 (2011) [arXiv:1101.1980 [hep-th]].

- [10] H. Singh, “Lifshitz/Schrödinger Dp-branes and dynamical exponents,” JHEP **1207**, 082 (2012) [arXiv:1202.6533 [hep-th]].
- [11] K. Narayan, “Lifshitz-like systems and AdS null deformations,” Phys. Rev. D **84**, 086001 (2011) [arXiv:1103.1279 [hep-th]].
- [12] D. Cassani and A. F. Faedo, “Constructing Lifshitz solutions from AdS,” JHEP **1105**, 013 (2011) [arXiv:1102.5344 [hep-th]].
- [13] W. Chemissany and J. Hartong, “From D3-Branes to Lifshitz Space-Times,” Class. Quant. Grav. **28**, 195011 (2011) [arXiv:1105.0612 [hep-th]].
- [14] N. Iizuka, N. Kundu, P. Narayan and S. P. Trivedi, “Holographic Fermi and Non-Fermi Liquids with Transitions in Dilaton Gravity,” JHEP **1201**, 094 (2012) [arXiv:1105.1162 [hep-th]].
- [15] W. Song and A. Strominger, “Warped ADS3/Dipole-CFT Duality”, arXiv:1109.0544 [hep-th].
- [16] G. T. Horowitz and B. Way, “Lifshitz Singularities,” arXiv:1111.1243 [hep-th].
- [17] N. Izhaki, J. Maldacena, J. Sonnenschein and S. Yankilowicz, Phys. Rev. **D58** (1998) 046004, [arXiv:9802042[hep-th]].
- [18] N. Ogawa, T. Takayanagi and T. Ugajin, “Holographic Fermi Surfaces and Entanglement Entropy,” JHEP **1201**, 125 (2012) [arXiv:1111.1023 [hep-th]].
- [19] L. Huijse, S. Sachdev and B. Swingle, “Hidden Fermi surfaces in compressible states of gauge-gravity duality,” Phys. Rev. B **85**, 035121 (2012) [arXiv:1112.0573 [cond-mat.str-el]].
- [20] K. Narayan, ‘On Lifshitz scaling and hyperscaling violation in string theory’, arXiv:1202.5935 [hep-th].
- [21] Bom Soo Kim, ‘Schrödinger Holography with and without Hyperscaling Violation’, arXiv:1202.6062v1 [hep-th].
- [22] P. Dey and S. Roy, “Lifshitz-like space-time from intersecting branes in string/M theory,” JHEP **1206**, 129 (2012) [arXiv:1203.5381 [hep-th]].
- [23] H. Lu, Y. Pang, C. N. Pope and J. F. Vazquez-Poritz, “AdS and Lifshitz Black Holes in Conformal and Einstein-Weyl Gravities,” Phys. Rev. D **86**, 044011 (2012) [arXiv:1204.1062 [hep-th]].

- [24] M. Alishahiha and H. Yavartanoo, “On Holography with Hyperscaling Violation,” JHEP **1211**, 034 (2012) [arXiv:1208.6197 [hep-th]].
- [25] M. Alishahiha, E. O Colgain and H. Yavartanoo, “Charged Black Branes with Hyperscaling Violating Factor,” JHEP **1211** (2012) 137 [arXiv:1209.3946 [hep-th]].
- [26] J. Gath, J. Hartong, R. Monteiro and N. A. Obers, ‘Holographic Models for Theories with Hyperscaling Violation,” arXiv:1212.3263 [hep-th].
- [27] K. Narayan, T. Takayanagi and S. P. Trivedi, “AdS plane waves and entanglement entropy,” JHEP **1304**, 051 (2013) [arXiv:1212.4328 [hep-th]]; K. Narayan, “Non-conformal brane plane waves and entanglement entropy,” arXiv:1304.6697 [hep-th].
- [28] M. Edalati and J. F. Pedraza, “Aspects of Current Correlators in Holographic Theories with Hyperscaling Violation,” arXiv:1307.0808 [hep-th].
- [29] C. Keeler, G. Knodel and J. T. Liu, “What do non-relativistic CFTs tell us about Lifshitz spacetimes?,” arXiv:1308.5689 [hep-th].
- [30] S. Ryu and T. Takayanagi, ”Aspects of Holographic Entanglement Entropy”, JHEP 0608 (2006) 045, [arXiv:0605073[hep-th]]; S. Ryu and T. Takayanagi, Phys. Rev. Lett. **86** (2006) 181602, [arXiv:0603001[hep-th]].
- [31] J. Maldacena and L. Susskind, “Cool horizons for entangled black holes,” arXiv:1306.0533 [hep-th].
- [32] T. Faulkner, A. Lewkowycz and J. Maldacena, “Quantum corrections to holographic entanglement entropy,” arXiv:1307.2892 [hep-th].
- [33] H. Singh, ”Lifshitz to AdS flow with interpolating p -brane solutions”, JHEP 1308 (2013) 097, [arXiv:1305.3784[hep-th]]